

Manuscript Details

Manuscript number	YJFLS_2016_682
Title	Gust Analysis using Computational Fluid Dynamics Derived Reduced Order Models
Article type	Research Paper

Abstract

Time domain gust response analysis based on large order nonlinear aeroelastic models is computationally expensive. An approach to the reduction of nonlinear models for gust response prediction is presented in this paper. The method uses information on the eigenspectrum of the coupled system Jacobian matrix and projects the full order model, through a series expansion, onto a small basis of eigenvectors which is capable of representing the full order model dynamics. The novelty in the paper concerns the representation of the gust term in the reduced model in a manner consistent with standard synthetic gust definitions, allowing a systematic investigation of the influence of a large number of gust shapes without regenerating the reduced model. Results are presented for the Goland wing/store configuration.

Keywords	aeroelasticity; gust analysis; computational fluid dynamics; reduced order model; worst case gust; Goland wing
Corresponding Author	Andrea Da Ronch
Corresponding Author's Institution	University of Southampton
Order of Authors	Andrea Da Ronch, Sebastian Timme, Kenneth Badcock
Suggested reviewers	gang chen, marcello righi, Daniella Raveh

Submission Files Included in this PDF

File Name [File Type]

2017-02-07-JFS-ResponseToReviewers.pdf [Response to Reviewers]

2017-02-07-Submitted.pdf [Manuscript File]

To view all the submission files, including those not included in the PDF, click on the manuscript title on your EVISE Homepage, then click 'Download zip file'.

1
2
3
4 **Gust Analysis using Computational Fluid Dynamics Derived Reduced Order**
5
6 **Models**

7
8
9 **Response to reviewers' comments**

10
11
12 We thank the reviewers for their time and comments about the manuscript. We are
13 pleased to see that all reviewers felt it is an interesting and novel work. We will
14 concentrate in the remainder of this response on the comments raised by the reviewers.
15
16
17

18
19
20 **Reviewer #1**

21 The article is about the reduction of nonlinear models for gust load prediction. The
22 method is capable of reducing the computational time and searching the worst case gust
23 at no additional costs. I think there are minor issues that have to be addressed before the
24 paper publication.
25
26
27

28
29
30 **Comment #1**

31
32 P.9: in Eq.(15), t_0 is time dimension and l_g is length dimension, please define the
33 relationship between time and length.
34

35
36 **Response**

37 The equation appearing in the initial submission was incorrect and has now been
38 reformulated in the revised manuscript as follows:
39

40
41
42
$$\dot{z}(t) = \frac{w_{g0}}{2} \left(1 - \cos \left(\frac{2\pi}{H_g} (t - t_0) \right) \right) \quad \text{for } t_0 < t < t_0 + H_g \quad (15)$$

43
44

45 We have also edited the text to account for this change, starting at line 131.
46
47

48
49
50 **Comment #2**

51 P.14, line 227: please define the form of gust vector, r
52

53
54 **Response**

55 We thank the reviewer for the comment and for the possibility that this comment gave
56
57
58
59

60
61
62 us to check the correctness of the statement. As discussed in the manuscript, lines
63 220-240, the term γ is a matrix as also evident from Eq. 29. We have therefore
64
65 corrected the initial statement to account for this.
66
67
68
69

70 **Comment #3**

71
72 P.18: table 1, what's the response time of full order calculation and ROM, in other
73 words, which response?
74

75 **Response**

76
77 CPU times in Table 1 are normalised by the CPU time needed to run an unsteady
78 CFD/CSD analysis. This allows presenting information which is independent from the
79 technical specifications of the computer machines used. We have applied no changes as
80 this point was already addressed in lines 279-281 of the original manuscript.
81
82
83
84
85

86 **Reviewer #2**

87
88 The paper presents the derivation of ROMs including both aerodynamics, structure
89 (modal representation) and a gust-type perturbation which is introduced as a grid
90 motion term. This represents an extension of Ref [16], it is very interesting and very
91 well presented.
92
93
94
95
96

97 **Comment #1**

98
99 On the negative side, the paper only presents one example (although it is relevant and
100 well described).
101

102 A second example would provide a significant added value.

103
104 **Response**

105
106 We have decided to discuss one test case only to produce a concise manuscript that
107 focuses on the novel aspect of the work. It is evident that all reviewers agree on the
108 interesting aspects of the method. Refs. 7, 10 and 11 present other test cases, and to
109 keep the manuscript concise we have edited the text to direct the reader to these
110 references for more information on other test cases. In particular, the revised
111 manuscript now contains in line 247:
112
113
114
115
116
117
118

119
120
121
122 *“For conciseness, the test case is for the Goland wing. Other test cases may be*
123 *found in the references herein provided. In particular, the interested reader is*
124 *referred to Ref. (7) for the initial investigation on a wing typical section, Ref. (10)*
125 *regarding a three-dimensional wing test case, and Ref. (11) for the extension to a*
126 *passenger transport aircraft.”*
127
128
129
130
131

132
133 **Comment #2**

134 More specifically, I have the following comments: the (in)dependence of the ROM
135 generating process on initial CFD flowfields is not explicitly stated, Ref [16] is slightly
136 more detailed but maybe the point should be expanded for the benefit of the reader not
137 familiar with such processes;
138
139
140

141 **Response**

142 The revised manuscript has been edited in line 171:

143
144
145 *“Finally, it is worth observing that the generation of the ROM is independent from*
146 *the initial equilibrium point. The coefficients of the ROM, however, depend on the*
147 *steady-state solution used in the generation process.”*
148
149
150
151

152
153 **Comment #3**

154 I am also missing a more general discussion of the implication of the various
155 assumptions and approximations vis-a-vis the accuracy of the solution; Ref [16] is a bit
156 more generous for instance,
157
158

159 **Response**

160 The revised manuscript has been edited starting from line 232:

161
162
163 *“Before proceeding to analyse the computational cost and general predictive*
164 *capabilities of the reduced model, considerations are given about the underlying*
165 *assumptions. First, the linear reduced order model is as accurate as the nonlinear*
166 *coupled solver in the limiting case that the response is small around the reference*
167 *equilibrium. With second order effects dominant, that are characterised, for*
168 *example, by strong moving shocks and large structural deformations, the*
169 *predictions will degrade. Second, the model projection relies on a dominant*
170
171
172
173
174
175
176
177

178
179
180
181 *subspace of coupled modeshapes that reproduce the relevant dynamics of the full*
182 *model. If needed, the basis for projection may be enriched by selection of*
183 *additional modeshapes. The last consideration is about the Schur complement*
184 *eigenvalue problem. This approach overcomes the limitation of the standard p--k*
185 *method, which is valid for undamped vibrations, because it provides a correct*
186 *identification of the aeroelastic damping using linearised CFD aerodynamics."*
187
188
189
190
191

192
193 **Comment #4**

194
195 provide references, if available, to application of the method to NS equation and/or
196 present all possible implications (finer grid, NS Jacobians, smaller time step),
197

198
199 **Response**

200 The revised manuscript has been edited in line 282:

201
202 *"A recent application to a viscous simulation is reported in Ref. (17)."*
203
204
205

206
207 **Comment #5**

208 is the "badness" of the response assessed on the basis of the tip displacement only? is
209 twist also taken into account? is bending moment also taken into account?
210

211
212 **Response**

213 Figures 4 and 5 show the vertical displacement at two points located at the wing tip as
214 well as the wing tip twist. The paper does not report the results in the typical shear,
215 moment, torsion (SMT) approach, which can be calculated as a post-processing
216 operation given the loads distribution along the wing.
217
218
219
220

221
222 **Comment #6**

223 can the sensitivity of the model to grid quality be assessed?
224

225
226 **Response**

227 The ROM is as good as the full order model, no matter the grid quality. Our work
228 focuses on the reduction of a given full order model (including uncertainties due to grid
229 refinement, numerical scheme, etc.). This does not matter for the ROM results: the task
230 of the ROM is to reproduce the reference as precisely as possible.
231
232
233
234
235
236

237
238
239
240
241 **Reviewer #3**

242
243 The paper expands a CFD-based ROM methodology that was formulated for stability
244 analysis to produce a ROM for gust response analysis. The ROM is demonstrated on
245 the Goland wing case, computing gust responses to gusts of various lengths. Linear and
246 nonlinear ROMs are formulated, but only the linear ROM is demonstrated with
247 numerical example. The formulation of the ROM is clear, but the results presented are
248 insufficient to substantiate it.
249
250
251
252
253

254
255 **Comment #1**

256
257 Validate the ROM methodology by presenting full CFD and ROM responses to gusts of
258 various profiles, and specifically to a sharp-edge gust on a 2D airfoil.
259
260

261 **Response**

262
263 For brevity and conciseness, we have included a three-dimensional test case only. The
264 reviewer's suggestion has already been investigated in Ref. (7) of the manuscript. That
265 work investigated the response to a sharp-edge gust, and compared the CFD-based
266 predictions with those obtained from a linear unsteady aerodynamic model. The reader
267 is referred to that work in various parts of the manuscript.
268
269
270
271
272

273
274 **Comment #2**

275
276 The name of manuscript doesn't reflect the content. Gust loads are not calculated in the
277 paper.
278

279 **Response**

280
281 This is correct and we have now removed the word 'load' from the initial title and from
282 the Abstract.
283
284
285

286
287 **Comment #3**

288
289 Present differences between full CFD and ROM in figure 4 as percentages of the full
290 CFD response value. From figure 4 they don't seem to be in "close agreement", as the
291 authors refer to them.
292
293
294
295

296
297
298
299 **Response**

300 The revised manuscript has been edited in line 308:

301
302 *“A good agreement, for the purpose of rapid engineering simulations, ...”*
303
304

305
306 **Comment #4**

307
308 Figure 5 only shows time responses to gusts of $L_g \leq 270$ that don't represent the worst
309 case gust response.
310

311 **Response**

312
313 We have added the response to gusts of length between 180 and 540 ft in Figure 5,
314 addressing the reviewer's comment.
315
316
317

318
319 **Comment #5**

320 Line 52, extra word 'and'.
321

322 **Response**

323
324 We have edited the manuscript accordingly along with other spelling mistakes we have
325 found proof reading the revised manuscript.
326
327
328
329
330
331
332
333
334
335
336
337
338
339
340
341
342
343
344
345
346
347
348
349
350
351
352
353
354

1
2
3
4
5
6
7
8
9
10
11
12
13
14
15
16
17
18

Gust Analysis using Computational Fluid Dynamics Derived Reduced Order Models

S. Timme^{a,1}, K. J. Badcock^{a,2}, and A. Da Ronch^{b,3,*}

^a*School of Engineering, University of Liverpool, Liverpool L69 3BX, U.K.*

^b*Faculty of Engineering and the Environment
University of Southampton, Southampton SO17 1BJ, U.K.*

Abstract

21
22
23
24
25
26
27
28
29
30
31
32
33
34
35
36
37
38
39
40
41
42
43

Time domain gust response analysis based on large order nonlinear aeroelastic models is computationally expensive. An approach to the reduction of nonlinear models for gust response prediction is presented in this paper. The method uses information on the eigenspectrum of the coupled system Jacobian matrix and projects the full order model, through a series expansion, onto a small basis of eigenvectors which is capable of representing the full order model dynamics. The novelty in the paper concerns the representation of the gust term in the reduced model in a manner consistent with standard synthetic gust definitions, allowing a systematic investigation of the influence of a large number of gust shapes without regenerating the reduced model. Results are presented for the Goland wing/store configuration.

Keywords: Aeroelasticity, Gust Analysis, CFD, Reduced Order Model, Worst Case Gust, Goland Wing

*Corresponding author. Email: A.Da-Ronch@soton.ac.uk

¹Lecturer. Member AIAA.

²Professor. Senior member AIAA.

³Lecturer. Member AIAA and AIAA Atmospheric Flight Mechanics Technical Committee.

1 **1. Introduction**

2 Aircraft regularly encounter atmospheric turbulence, inducing changes
3 in forces and moments, which cause rigid and flexible dynamic responses.
4 These responses introduce loads on the structure which must be accounted
5 for during the design stage to ensure structural integrity. The turbulence is
6 regarded, for linear analysis, as a set of component velocities (gusts) super-
7 imposed on the background steady flow. The loads encountered form some of
8 the critical cases used in the structural sizing of a passenger jet. The capabil-
9 ity to calculate design loads with a high degree of accuracy would potentially
10 allow reduced conservatism without compromising safety. Currently, conser-
11 vatism is necessary because of the limited certainty of the possible forms of
12 atmospheric gusts and the limited realism for some flow regimes of linear
13 methods used to predict the aircraft response.

14 The well-established methods for gust load calculations are based on lin-
15 ear aerodynamic models which are solved in the frequency domain. The use
16 of high-fidelity models based on computational fluid dynamics (CFD) in the
17 research setting has been reported, for example, in Ref. (1). Grid veloci-
18 ties are used to apply a disturbance in a time domain CFD calculation (2),
19 overcoming the problems associated with numerical dissipation of the distur-
20 bance but also missing the influence of the aircraft flow field and motion on
21 the gust.

22 The cost of time domain calculations makes the routine use of CFD in
23 gust response analysis impractical, and system-identification methods have
24 been used as a cheaper alternative. Proper orthogonal decomposition has

113
114
115
116
117
118
119
120 25 been used as a model reduction technique (3) to generate reduced models
121 26 for gust simulations, but this method suffers from the usual limitations as-
122
123 27 sociated with the necessity for a set of training data closely related to the
124
125 28 final application cases, and the difficulty of accounting for nonlinearity in
126
127 29 the reduced model. A systematic and cost effective approach to developing
128
129 30 reduced models capable of describing both linear and nonlinear effects for a
130
131 31 range of cases based on limited development cost has, to date, proved elusive.

132 An approach to calculating a reduced order model from a large dimension
133 33 CFD model which can calculate a nonlinear response has been reviewed in
134
135 34 Ref. (4). The method first calculates the important modes of the problem
136
137 35 from a large order eigenvalue problem. For an aeroelastic limit-cycle oscilla-
138
139 36 tion (LCO), the system responds in the critical mode close to the bifurcation
140
141 37 point. The approach presented in Refs. (5; 6) is to project the full order
142
143 38 model onto the critical mode and expand the residual in a Taylor series, re-
144
145 39 taining quadratic and cubic terms. The influence of the non-critical space
146
147 40 on the critical mode is included through a centre manifold approximation.
148
149 41 The method has been successfully applied to various test cases, including
150
151 42 the LCO prediction dominated by the motion of a shock wave (5) and a
152
153 43 prototype flight dynamics instability of a delta wing (6). The approach to
154
155 44 model reduction has been generalized in Ref. (7) by using multiple coupled
156
157 45 system eigenmodes for model projection and introducing control deflection
158
159 46 and gust interaction effects in the formulation. Reference (8) introduced the
160
161 47 flight mechanics degrees of freedom to predict the dynamics of flexible flying
162
163 48 aircraft. The method has several strengths, namely: (i) it exploits informa-
164
165 49 tion from the stability (flutter) calculation for the development of a reduced
166
167
168

169
170
171
172
173
174
175
176 50 order model (ROM) for dynamic response analyses; (ii) linear or nonlinear
177 51 reduced models can be developed within the same framework; (iii) the re-
178 52 duced model can be parameterised to avoid ROM regeneration; and (iv) the
180 53 ROM in state–space form is suitable for control design studies.

182 54 The current paper tackles the problem of how to introduce gust terms
183 55 into the reduced model to allow a gust load analysis to be carried out. The
185 56 objective is to develop a methodology that allows the reduced model to con-
187 57 sider a whole range of gust excitations without recourse to the full order
189 58 model. The outgrowth of this work is the capability to carry out the search
190 59 of the worst case gust at no additional costs than those initially encountered
192 60 in generating the reduced model.

194 61 The paper continues with the formulation of the full order aeroelastic
195 62 model in Sec. 2. The procedure to obtain a reduced model is discussed in
197 63 Sec. 3. Then a new approach to calculating the gust term in the ROM is
199 64 proposed. Results are then given in Sec. 4 for a test case to evaluate the
200 65 method from the point of view of accuracy and computational efficiency.
202 66 Finally, conclusions are drawn in Sec. 5. The important features of the
204 67 method developed are: (i) linear and nonlinear ROMs can be derived; and
206 68 (ii) the model reduction is performed once, with application of any gust made
207 69 without further recourse to the CFD code.

70 **2. Full Order Model**

212 71 The Euler equations are solved in the curvilinear form on block–structured
214 72 body–conforming grids:

$$\frac{\partial \hat{\mathbf{W}}}{\partial t} + \frac{\partial \hat{\mathbf{F}}}{\partial \xi} + \frac{\partial \hat{\mathbf{G}}}{\partial \eta} + \frac{\partial \hat{\mathbf{H}}}{\partial \zeta} = 0 \quad (1)$$

The transformation from Cartesian coordinates defines a curvilinear coordinate system from:

$$\xi = \xi(x, y, z, t), \quad \eta = \eta(x, y, z, t), \quad \zeta = \zeta(x, y, z, t) \quad (2)$$

with the Jacobian determinant of the transformation given by:

$$J = \left| \frac{\partial(\xi, \eta, \zeta)}{\partial(x, y, z)} \right|. \quad (3)$$

The conserved variables, $\hat{\mathbf{W}}$, and the flux vectors, $\hat{\mathbf{F}}$, $\hat{\mathbf{G}}$ and $\hat{\mathbf{H}}$, are then defined as follows:

$$\hat{\mathbf{W}} = \frac{1}{J} \mathbf{W} \quad (4)$$

$$\hat{\mathbf{F}} = \frac{1}{J} (\xi_x \mathbf{F} + \xi_y \mathbf{G} + \xi_z \mathbf{H}) \quad (5)$$

$$\hat{\mathbf{G}} = \frac{1}{J} (\eta_x \mathbf{F} + \eta_y \mathbf{G} + \eta_z \mathbf{H}) \quad (6)$$

$$\hat{\mathbf{H}} = \frac{1}{J} (\zeta_x \mathbf{F} + \zeta_y \mathbf{G} + \zeta_z \mathbf{H}) \quad (7)$$

where the subscripts \bullet_x , \bullet_y and \bullet_z denote differentiation with respect to x , y and z , respectively. The terms \mathbf{F} , \mathbf{G} and \mathbf{H} are given by:

$$\mathbf{W} = [\rho, \rho u, \rho v, \rho w, \rho E]^T \quad (8)$$

$$\mathbf{F} = [\rho u, \rho u^2 + p, \rho uv, \rho uw, u(\rho E + p)]^T \quad (9)$$

$$\mathbf{G} = [\rho v, \rho uv, \rho v^2 + p, \rho vw, v(\rho E + p)]^T \quad (10)$$

$$\mathbf{H} = [\rho w, \rho uw, \rho vw, \rho w^2 + p, w(\rho E + p)]^T. \quad (11)$$

281
 282
 283
 284
 285
 286
 287
 288
 289
 290
 291
 292
 293
 294
 295
 296
 297
 298
 299
 300
 301
 302
 303
 304
 305
 306
 307
 308
 309
 310
 311
 312
 313
 314
 315
 316
 317
 318
 319
 320
 321
 322
 323
 324
 325
 326
 327
 328
 329
 330
 331
 332
 333
 334
 335
 336

80 The Euler equations are discretised on curvilinear multiblock body-conforming
 81 grids using a cell-centered finite-volume method. The residual is formed us-
 82 ing Osher's approximate Riemann solver with the monotone upwind scheme
 83 for conservation laws interpolation. Exact Jacobian matrices are formed.
 84 The mesh can be deformed using transfinite interpolation. More details on
 85 the CFD formulation can be found in Ref. (9), and on the application to
 86 problems in aeroelasticity in Ref. (4).

87 As given in Ref. (4), for general linear structural motions, the dimen-
 88 sionless structural equations of motion are defined in physical coordinates
 89 as:

$$\mathbf{M}\delta\ddot{\mathbf{x}}_s + \mathbf{C}\delta\dot{\mathbf{x}}_s + \mathbf{K}\delta\mathbf{x}_s = \vartheta \mathbf{f}. \quad (12)$$

90 The deflections $\delta\mathbf{x}_s$ of the (linear) structure are defined at the set of physical
 91 coordinates \mathbf{x}_s by $\delta\mathbf{x}_s = \mathbf{\Xi} \boldsymbol{\eta}$, where the vector $\boldsymbol{\eta}$ contains the generalised
 92 coordinates (modal amplitudes). The columns of the matrix $\mathbf{\Xi}$ contain the
 93 mode shape vectors evaluated from a finite-element model of the structure
 94 with the deflections defined at the structural grid points. Projecting the
 95 finite-element equations onto the mode shapes, while scaling to obtain gen-
 96 eralised masses of magnitude one (i.e. $\mathbf{\Xi}^T \mathbf{M} \mathbf{\Xi} = \mathbf{I}$, with \mathbf{I} as the identity

337 matrix) gives a system of scalar equations written in state-space with the
 338
 339
 340
 341
 342
 343
 344
 345 structural residual given by:
 346
 347

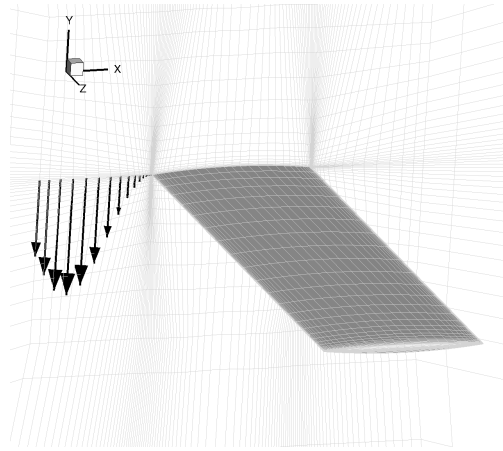
$$348 \quad \mathbf{R}_s = \begin{bmatrix} \mathbf{0} & \mathbf{I} \\ -\boldsymbol{\Xi}^T \mathbf{K} \boldsymbol{\Xi} & -\boldsymbol{\Xi}^T \mathbf{C} \boldsymbol{\Xi} \end{bmatrix} \mathbf{w}_s + \begin{bmatrix} \mathbf{0} \\ \mathbf{I} \end{bmatrix} \vartheta \boldsymbol{\Xi}^T \mathbf{f} \quad (13)$$

349
 350
 351
 352
 353 and the vector of structural unknowns $\mathbf{w}_s = [\boldsymbol{\eta}^T, \dot{\boldsymbol{\eta}}^T]^T$ containing the gener-
 354 alised coordinates and their velocities. The vector \mathbf{f} of aerodynamic forces
 355 (pressure) at the structural grid points follows from the wall pressure, the
 356 area of the surface segment and the unit normal vector, and thus is a function
 357 of fluid and structural unknowns. It is then projected using the mode shapes
 358 to obtain the generalised forces $\boldsymbol{\Xi}^T \mathbf{f}$. The parameter ϑ for the mass ratio
 359 is obtained from the nondimensionalisation of the governing equations, and
 360 depends on the reference density and the reference length. The method used
 361 to transfer the surface pressure forces to the structural nodes is described in
 362 Ref. (4).
 363
 364
 365
 366
 367
 368
 369
 370

371 2.1. Gust Representation

372
 373 Synthetic gusts are defined by space-time functions of a velocity distur-
 374 bance that propagates through the flow field, interacting with the aircraft. In
 375 principle, these disturbances can be introduced through the far field bound-
 376 ary conditions, with the propagation done within the CFD solution. In prac-
 377 tice, the gust disturbance will be dissipated by the discretisation. As an alter-
 378 native, assuming that the gust disturbance propagates without being altered
 379 by the background flow field and interaction, a frozen gust can be applied
 380 by introducing the gust disturbance through additional contributions to the
 381
 382
 383
 384
 385
 386

393
 394
 395
 396
 397
 398
 399
 400 mapping velocity terms ξ_t , η_t and ζ_t in Eqs. (8)–(11). The flow variables are
 401 then altered in the discretised version of Eq. (1) through the resulting terms
 402 in the fluxes. This approach has been successfully demonstrated for CFD
 403 based gust analysis. A schematic in Fig. 1 shows the progressive application
 404 of the gust to the grid velocities.
 405
 406
 407



408
 409
 410
 411
 412
 413
 414
 415
 416
 417
 418
 419
 420
 421
 422 Figure 1: Demonstration of gust application to the CFD; the arrows indicate the grid
 423 velocity at each point for a gust of length 6 ft; only the points on the symmetry plane for
 424 $z = 0$ are shown
 425
 426

427
 428 The disturbances used in this framework are of the discrete and contin-
 429 uous types, see for example Refs. (10; 11). For the vertical component of a
 430 discrete gust, for example, the disturbance at each grid point is defined by:
 431
 432
 433

$$\dot{\mathbf{z}}(t) = \mathbf{f}(\mathbf{x}, t) \quad (14)$$

434
 435
 436
 437
 438 where $\dot{\mathbf{z}}$ is the vector of the vertical component of the mesh velocities, \mathbf{f} is
 439 the function defining these velocities, depending on the mesh point location,
 440
 441
 442

449
 450
 451
 452
 453
 454
 455
 456 128 \mathbf{x} , and the time instant, t . For example, a discrete one-minus-cosine gust,
 457 129 for a single mesh point, is given by:

$$460 \quad \dot{z}(t) = \frac{w_{g0}}{2} \left(1 - \cos \left(\frac{2\pi}{H_g} (t - t_0) \right) \right) \quad \text{for } t_0 < t < t_0 + H_g \quad (15)$$

461
 462
 463
 464 130
 465
 466 131 where t_0 is the **nondimensional** time at which the gust is set to begin, w_{g0}
 467
 468 132 is the gust intensity, and H_g is the **nondimensional** gust length ($H_g = L_g/c$
 469
 470 133 **where L_g is the gust length and c is a characteristic length**). In this paper,
 471
 472 134 the gust disturbance applied to each grid point in the mesh is defined as:

$$473 \quad \mathbf{u}_d = [\dots, \dot{x}, \dot{y}, \dot{z}, \dots]^T \quad (16)$$

474
 475
 476
 477
 478 135 with one triplet of \dot{x} , \dot{y} and \dot{z} for each mesh point.

481 136 **3. Model Reduction**

482
 483 137 The full order nonlinear aeroelastic model is written in semi-discrete form.
 484
 485 138 Denote by \mathbf{w} the n -dimensional state-space vector arising from the fluid and
 486
 487 139 structural spatial discretisation, which is conveniently partitioned into fluid
 488
 489 140 and structural degrees of freedom:

$$490 \quad \mathbf{w} = [\mathbf{w}_f^T, \mathbf{w}_s^T]^T. \quad (17)$$

491
 492
 493
 494
 495 141 The state-space equations in the general vector form are:

$$\frac{d\mathbf{w}}{dt} = \mathbf{R}(\mathbf{w}, \mathbf{u}_d) \quad (18)$$

where $\mathbf{R} = [\mathbf{R}_f^T, \mathbf{R}_s^T]$ is the (nonlinear) residual and \mathbf{u}_d is a vector denoting the applied gust disturbance acting on the system. The homogeneous system has an equilibrium solution, \mathbf{w}_0 , for a given constant \mathbf{u}_{d0} , corresponding to a constant solution in the state–space and satisfying the aeroelastic equilibrium equation:

$$\frac{d\mathbf{w}_0}{dt} = \mathbf{R}(\mathbf{w}_0, \mathbf{0}) = \mathbf{0}. \quad (19)$$

The system often also includes an independent parameter (freestream speed, air density, altitude, etc.) which is varied to study stability of the equilibria.

Denote by $\Delta\mathbf{w} = \mathbf{w} - \mathbf{w}_0$ the increment in the state–space vector with respect to an equilibrium solution (12). The large order nonlinear residual formulated in Eq. (18) is expanded in a Taylor series around the equilibrium point:

$$\mathbf{R}(\mathbf{w}) \approx \mathbf{A} \Delta\mathbf{w} + \frac{\partial \mathbf{R}}{\partial \mathbf{u}_d} \Delta\mathbf{u}_d + \frac{1}{2} \mathbf{B}(\Delta\mathbf{w}, \Delta\mathbf{w}) + \frac{1}{6} \mathbf{C}(\Delta\mathbf{w}, \Delta\mathbf{w}, \Delta\mathbf{w}) \quad (20)$$

retaining terms up to third order in the perturbation variable. The treatment of the gust term, which appears as the second term on the right hand side, is considered below. The Jacobian matrix of the coupled system is denoted as \mathbf{A} , and the vectors \mathbf{B} and \mathbf{C} indicate, respectively, the second and third order derivative operators. The full order system is projected onto a basis formed by a small number (denoted by m) of eigenvectors of the Jacobian

561
562
563
564
565
566
567
568 matrix evaluated at the equilibrium position. Right and left eigenvectors are
569 scaled to satisfy the biorthonormality conditions (7). The projection of the
570 full-order model is done using a transformation of coordinates:
571
572
573

$$574 \quad \Delta \mathbf{w} = \mathbf{\Phi} \mathbf{z}_c + \bar{\mathbf{\Phi}} \bar{\mathbf{z}}_c \quad (21)$$

577 where $\mathbf{z}_c \in \mathbb{C}^m$ is the state-space vector governing the dynamics of the
578 reduced order nonlinear system, and $\mathbf{\Phi}$ is the matrix of right eigenvectors of
579 \mathbf{A} . The result is a system of ordinary differential equations in \mathbf{z}_c which have
580 linear, quadratic and cubic terms in \mathbf{z}_c . The coefficients of these terms are
581 derived by using matrix-free approximations for the first, second and third
582 order derivative operators applied to combinations of the columns of $\mathbf{\Phi}$ (i.e.
583 the basis vectors for the reduction). The matrix-free approximations work
584 on residual evaluations, but require extended order arithmetic to be used
585 to obtain accurate approximations. The full details of the methodology are
586 given in Refs. (5; 7; 12; 13).
587
588
589
590
591
592
593

594 In the current paper, the linear reduced model, obtained by neglecting the
595 terms \mathbf{B} and \mathbf{C} in Eq. (20), is generated for gust analysis. Substituting first
596 for $\Delta \mathbf{w}$ of Eq. (21) into Eq. (20), and then pre-multiplying by $\bar{\mathbf{\Psi}}^T$, which is
597 the matrix of left eigenvectors of \mathbf{A} , one obtains the linear ROM:
598
599
600

$$601 \quad \dot{\mathbf{z}}_c = \text{diag}(\lambda) \mathbf{z}_c + \bar{\mathbf{\Psi}}^T \frac{\partial \mathbf{R}}{\partial \mathbf{u}_d} \Delta \mathbf{u}_d \quad (22)$$

602
603
604 where $\text{diag}(\lambda)$ is a diagonal matrix of size $[m, m]$ containing the complex
605 eigenvalues corresponding to the eigenvectors used in the projection. Through
606 manipulation of the terms in \mathbf{B} and \mathbf{C} , a nonlinear ROM can be obtained if
607 required (7; 12).
608
609
610

617
618
619
620
621
622
623
624 171 Finally, it is worth observing that the generation of the ROM is inde-
625 172 pendent from the initial equilibrium point. The coefficients of the ROM,
626
627 173 however, depend on the steady-state solution used in the generation process.

628
629
630 174 *3.1. Nonlinear Eigenvalue Problem*

631
632 175 A major computational challenge arises, when using CFD as the source of
633 176 the aerodynamic predictions, to calculate the system eigenvectors. To over-
634
635 177 come this problem, the Schur complement eigenvalue formulation is used.
636
637 178 The coupled system Jacobian matrix of Eq. (18) is most conveniently ma-
638 179 nipulated by partitioning the matrix as

$$640 \quad \mathbf{A} = \begin{bmatrix} \frac{\partial \mathbf{R}_f}{\partial \mathbf{w}_f} & \frac{\partial \mathbf{R}_f}{\partial \mathbf{w}_s} \\ \frac{\partial \mathbf{R}_s}{\partial \mathbf{w}_f} & \frac{\partial \mathbf{R}_s}{\partial \mathbf{w}_s} \end{bmatrix} = \begin{bmatrix} \mathbf{A}_{ff} & \mathbf{A}_{fs} \\ \mathbf{A}_{sf} & \mathbf{A}_{ss} \end{bmatrix}. \quad (23)$$

645 180 The block \mathbf{A}_{ff} represents the influence of the fluid unknowns on the fluid
646 181 residual, and has by far the largest number of non-zeros for the structural
647
648 182 models used in this paper. The term \mathbf{A}_{fs} arises from the dependence of
649
650 183 the CFD residual on the mesh motion and speeds, which depend in turn on
651
652 184 the structural solution, and is evaluated by finite differences. The term \mathbf{A}_{sf}
653
654 185 is due to the dependence of the generalized forces on the surface pressures.
655
656 186 Finally, the block \mathbf{A}_{ss} is the Jacobian of the structural equations with respect
657 187 to the structural unknowns.

658 188 Write the coupled system eigenvalue problem as:

$$660 \quad \begin{bmatrix} \mathbf{A}_{ff} & \mathbf{A}_{fs} \\ \mathbf{A}_{sf} & \mathbf{A}_{ss} \end{bmatrix} \phi = \lambda \phi \quad (24)$$

673
674
675
676
677
678
679
680 where ϕ and λ are the complex eigenvector and eigenvalue, respectively.

681 Partition the eigenvector as:
682

$$\phi = \left[\phi_f^T, \phi_s^T \right]^T \quad (25)$$

683
684
685
686
687
688 In Eq. (24), substituting ϕ_f from the first set of equations into the second set
689 of equations, one finds that the eigenvalue λ , assuming it is not an eigenvalue
690 of \mathbf{A}_{ff} , satisfies the nonlinear eigenvalue problem:
691
692
693

$$\mathbf{S}(\lambda) \phi_s = \lambda \phi_s \quad (26)$$

694 where $\mathbf{S}(\lambda) = \mathbf{A}_{ss} - \mathbf{A}_{sf} (\mathbf{A}_{ff} - \lambda I)^{-1} \mathbf{A}_{fs}$. The matrix $\mathbf{S}(\lambda)$ is the sum of
695 the structural matrix and a second term arising from the coupling of the fluid
696 and structure. Equation (26), which is a nonlinear eigenvalue problem, is
697 solved using Newton's method. To overcome the cost of forming the residual
698 and its Jacobian matrix at each iteration, an approximation of $(\mathbf{A}_{ff} - \lambda I)^{-1}$
699 is used. The calculation of the left eigenvector ψ involves solving the adjoint
700 problem of Eq. (24). More details on the Schur complement eigenvalue solver
701 and its application to realistically sized aeroelastic models can be found in
702 Ref. (14).
703
704
705
706
707
708
709
710
711
712

713 3.2. Gust Term in the Reduced Order Model Setting

714
715 As described above, the gust is introduced into the full order model
716 through the grid velocities, represented in Eq. (18) by the vector \mathbf{u}_d . The
717 treatment of this component in the reduced model is the main contribution
718 of this paper. The challenge is to manipulate the term $\frac{\partial \mathbf{R}}{\partial \mathbf{u}_d} \Delta \mathbf{u}_d$ in Eq. (22)
719
720
721
722

729
730
731
732
733
734
735
736 so that it is represented in a convenient way in the reduced model. Using the
737 chain rule, the dependence of the nonlinear full order residual on the gust
738 perturbation is rewritten as:
739

$$740 \quad \frac{\partial \mathbf{R}}{\partial \mathbf{u}_d} = \frac{\partial \mathbf{R}}{\partial \mathbf{u}} \frac{\partial \mathbf{u}}{\partial \mathbf{u}_d} \quad (27)$$

741
742
743
744
745 where \mathbf{u} is a vector of mesh velocities. The first term on the right side depends
746 on mesh point velocities only and can be computed independently of the gust
747 definition using finite differences, analytical or automatic differentiation.
748
749

750 The second term on the right side of Eq. (27) depends on both spatial
751 and temporal coordinates. The reason for this is that, recalling Eq. (14),
752 the prescribed gust is in general a function of space and time. The gust
753 simulation using a ROM, as formulated in Refs. (7; 10), requires at each
754 time step the calculation of the contribution arising from
755
756
757

$$758 \quad \bar{\psi}^T \frac{\partial \mathbf{R}}{\partial \mathbf{u}} \frac{\partial \mathbf{u}}{\partial \mathbf{u}_d} \Delta \mathbf{u}_d. \quad (28)$$

759
760
761
762
763 The first two terms involve a matrix–matrix multiplication, and this can be
764 carried out once during the generation of the ROM calculation independently
765 of the gust definition. This defines a **matrix**, γ , which is constant and in-
766 dependent of the gust shape. The term $\frac{\partial \mathbf{u}}{\partial \mathbf{u}_d}$ is simply the identity matrix
767 when using the field velocity method to prescribe the gust, and \mathbf{u}_d is the
768 time varying vector defining the propagation in time and space of the gust
769 disturbances. At each time step iteration for solving the ROM, the vector on
770 the right side needs to be updated to account for the gust translation, and
771 a matrix–vector multiplication is then needed. It is worth noting that the
772
773
774
775
776
777
778

785
786
787
788
789
790
791
792 228 CFD code does not need to be accessed for this operation, which requires
793 229 only the grid point coordinates, and the ROM can be applied to any gust
794
795 230 shape (discrete and continuous).

796
797 231 The linear reduced model is then written as:

$$\dot{z}_c = \text{diag}(\lambda) z_c + \gamma^T \Delta \mathbf{u}_d \quad (29)$$

803 232 Before proceeding to analyse the computational cost and general predic-
804
805 233 tive capabilities of the reduced model, considerations are given about the
806
807 234 underlying assumptions. First, the linear ROM is as accurate as the nonlin-
808
809 235 ear coupled solver in the limiting case that the response is small around the
810
811 236 reference equilibrium. With second order effects dominant, that are charac-
812
813 237 terised, for example, by strong moving shocks and large structural deforma-
814
815 238 tions, the predictions will degrade. Second, the model projection relies on a
816
817 239 dominant subspace of coupled modeshapes that reproduce the relevant dy-
818
819 240 namics of the full model. If needed, the basis for projection may be enriched
820
821 241 by selection of additional modeshapes. The last consideration is about the
822
823 242 Schur complement eigenvalue problem. This approach overcomes the limi-
824
825 243 tation of the standard p-k method, which is valid for undamped vibrations,
826
827 244 because it provides a correct identification of the aeroelastic damping using
828
829 245 linearised CFD aerodynamics.

828 246 4. Results

830
831 247 For conciseness, the test case is for the Goland wing. Other test cases
832
833 248 may be found in the references herein provided. In particular, the interested

841
842
843
844
845
846
847
848 249 reader is referred to Ref. (7) for the initial investigation on a wing typical
849 250 section, Ref. (10) regarding a three-dimensional wing test case, and Ref. (11)
850
851 251 for the extension to a passenger transport aircraft.

852 The Goland wing has a chord of 6 ft and a span of 20 ft. It is a rectangular
853 cantilevered wing with a 4% thick parabolic section. The structural model for
854 253 the wing/store configuration follows the description given in Ref. (15). The
855
856 254 four mode shapes shown in Fig. 2 were retained for the aeroelastic simulations
857
858 255 herein presented. The CFD grid for Euler simulations has about 400,000
859
860 256 points. All simulations are done for a freestream Mach number of 0.85 and
861
862 257 one degree angle of attack chosen to allow the influence of static deformation
863
864 258 on the symmetric wing model.
865

866 First, a stability calculation was made using the Schur complement method
867
868 261 as in Ref. (16). The traces of the aeroelastic eigenvalues are shown in Fig. 3
869
870 262 as a function of the equivalent airspeed (EAS). One thousand altitude steps
871
872 263 for the altitude traces were employed. The wing model shows the typical
873
874 264 bending-torsion type of instability. The eigenvectors for the model reduc-
875
876 265 tion were computed at the subcritical altitude of 40,000 ft corresponding to
877
878 266 408 ft/s EAS.

879 Then, the ROM was calculated with the gust terms. Four aeroelastic
880
881 268 modes, corresponding to the four structural normal modes in Figure 2, were
882
883 269 used for the reduction. The coefficients of the linear reduced model, without
884
885 270 reporting the gust term, were found to be:

$$\dot{\mathbf{z}}_c = \text{diag}(\lambda_1, \lambda_2, \lambda_3, \lambda_4) \mathbf{z}_c \quad (30)$$

888
889 271 where $\lambda_1 = -1.636 \cdot 10^{-3} + 7.888 \cdot 10^{-2} i$, $\lambda_2 = -9.453 \cdot 10^{-3} + 1.209 \cdot 10^{-1} i$,

897
898
899
900
901
902
903
904
905
906
907
908
909
910
911
912
913
914
915
916
917
918
919
920
921
922
923
924
925
926
927
928
929
930
931
932
933
934
935
936
937
938
939
940
941
942
943
944
945
946
947
948
949
950
951
952

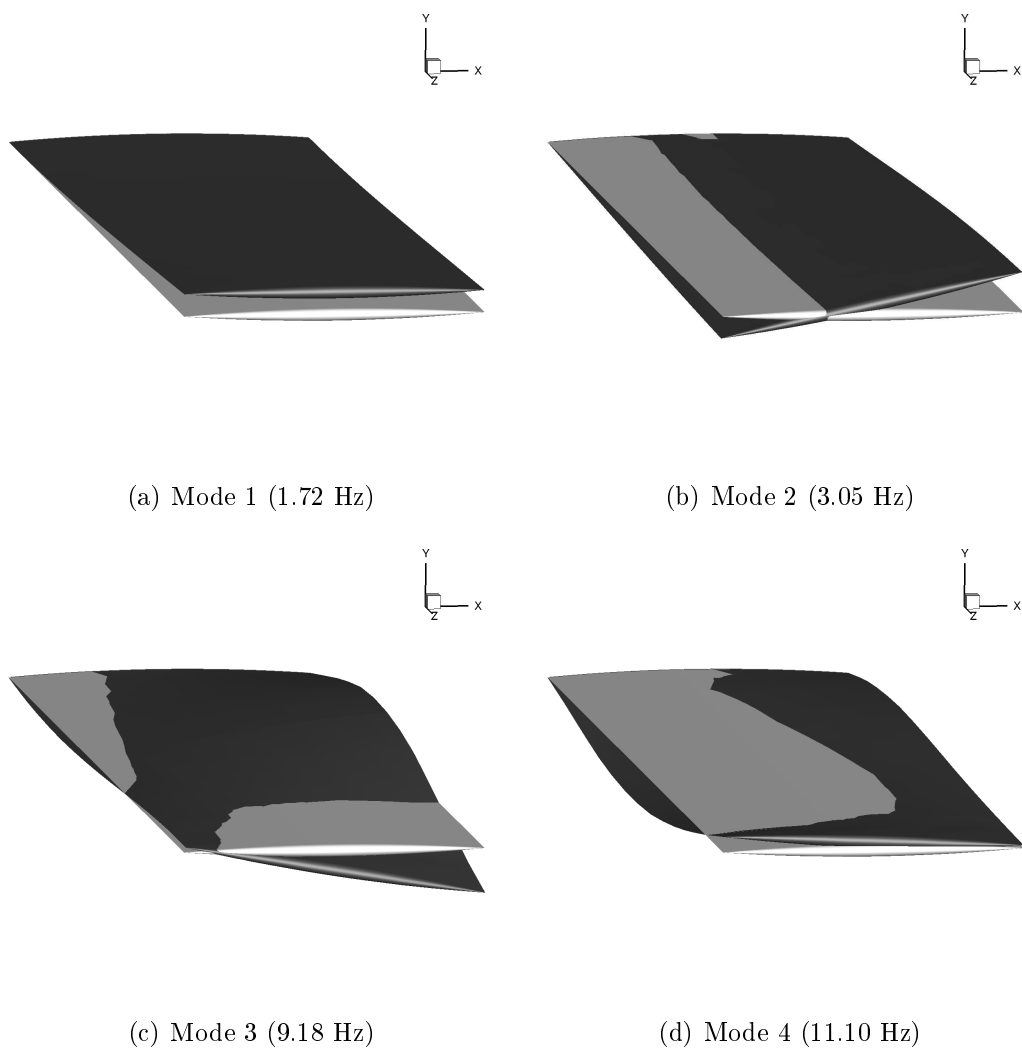


Figure 2: Modeshapes for the Goland wing/store configuration; for illustration purposes, a modal amplitude of 4 is used

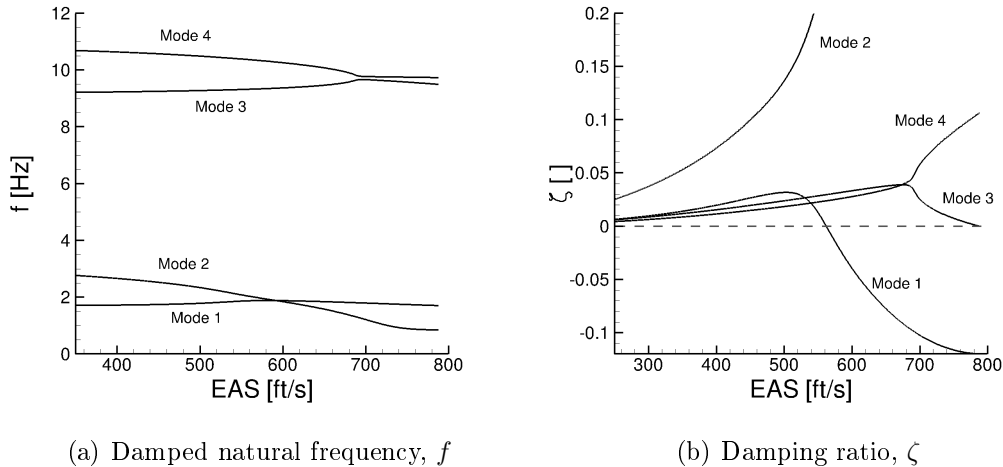


Figure 3: Eigenvalue traces for Goland wing/store configuration (Mach 0.85, one degree angle of attack)

272 $\lambda_3 = -5.027 \cdot 10^{-3} + 4.229 \cdot 10^{-1} i$, and $\lambda_4 = -7.716 \cdot 10^{-3} + 4.867 \cdot 10^{-1} i$.

273 Table 1 compares the computational efficiency of the reduced model
 274 against that of the full order model. All calculations, based on full and
 275 reduced models, were run on a single process of a 4-core Intel Xeon 3.3GHz
 276 computer, and a nondimensional time step of 0.01 was used. For compar-
 277 ison, computational costs were normalised by the cost of the time domain
 278 full order model. It is worth noting that smaller time steps would likely be
 279 required for viscous simulations, with longer time histories also needed to
 280 determine a response involving a wider range of frequencies. The reduced
 281 model generation times do not scale with these factors, and hence the tim-
 282 ings given in Table 1 are considered conservative. **A recent application to a**
 283 **viscous simulation is reported in Ref. (17).** Timings start from a precursor
 284 eigenvalue calculation which would be done as part of a flutter calculation.

1009
 1010
 1011
 1012
 1013
 1014
 1015
 285 The generation of the ROM, which consists of the eigenvector calculation and
 1016
 1017 the calculation of the gust term, γ , takes about 13% of the cost of the full
 286
 1018
 1019 order time response calculation. The time integration of the reduced model,
 1020
 1021 Eq. (29), is essentially free.
 288

Step	Cost
Time Domain Full Order Calculation	$1 \cdot 10^0$
Reduced Model Generation:	
a) Calculating Eigenvector Basis	$3 \cdot 10^{-2}$
b) Calculating Gust Vector, γ	$1 \cdot 10^{-1}$
Time Domain Reduced Model Calculation	$1 \cdot 10^{-5}$

1022
 1023
 1024
 1025
 1026
 1027
 1028
 1029
 1030
 1031
 1032
 1033
 1034 Table 1: Computational cost for the generation and use of the ROM for gust analysis
 1035
 1036

1037
 289 To illustrate the potential benefits of the reduced model, the worst case
 1038
 1039 gust search was carried out for the one-minus-cosine family of gusts. The
 290
 1040 wing response is characterised by the displacement at the wing tip leading
 291
 1041 and trailing edges, and the resulting twist of the wing tip. Figure 4 shows the
 1042
 1043 peaks of the response for different gust lengths computed by the full order
 1044
 293 (CFD) and reduced (ROM) models. The reduced model was generated once,
 1045
 1046 and then deployed for the worst case gust search at no additional costs. **A**
 294
 1047
 295
 1048
 296 **good agreement, for the purpose of rapid engineering simulations,** between
 1049
 1050 the reduced and full order predictions was found. The worst case gust is
 1051
 1052 for a gust length of approximately 400 ft at a speed of 408 ft/s EAS, which
 1053
 1054
 299 excites the response predominantly in the first bending mode (normal mode
 1055
 1056 at 1.72 Hz). The time responses for different gust lengths are shown in Fig. 5,
 300

1065
1066
1067
1068
1069
1070
1071
1072 301 and confirm the predictive general capabilities of the reduced model for gust
1073 302 response analysis.

1074 1075 1076 303 **5. Conclusions** 1077

1078
1079 304 The introduction of a gust into a reduced model in a manner consistent
1080 305 with well-established gust definitions has been considered. A new method
1081
1082 306 was proposed that allows a one-off model reduction, with any gust sub-
1083
1084 307 sequently applied to the reduced model. The formulation allows linear or
1085
1086 308 nonlinear reduced models to be derived, based on a range of full order mod-
1087
1088 309 elling options, including linear or nonlinear structural models, and linear or
1089
1090 310 CFD aerodynamic models. In the current paper, linear reduced models of
1091
1092 311 the CFD have proved adequate for the gust interaction simulations. Re-
1093
1094 312 sults were presented for a wing test case (Golang wing/store configuration)
1095
1096 313 to demonstrate the capability of the method. The ability of the method to
1097
1098 314 enable calculations for a variety of gusts was illustrated.

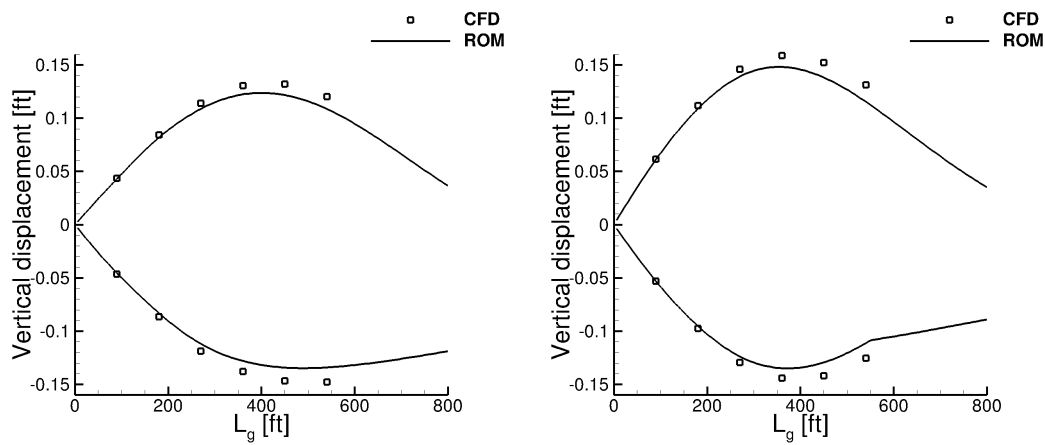
1098 1099 315 **Acknowledgments** 1100

1101
1102 316 This work was supported by the U.K. Engineering and Physical Sciences
1103
1104 317 Research Council (EPSRC) under grant EP/I014594/1.

1105 1106 318 **References** 1107

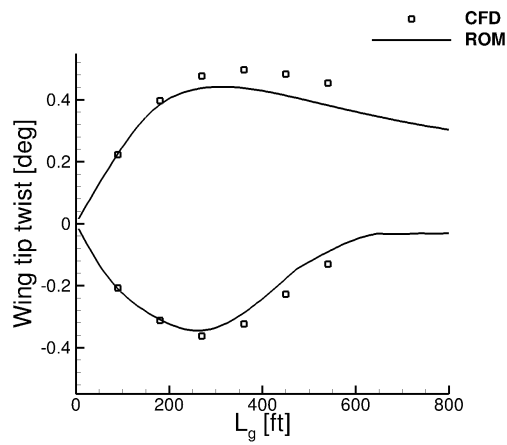
- 1108
1109 319 [1] D. E. Raveh, Gust-response analysis of free elastic aircraft in the
1110
1111 320 transonic flight regime, *Journal of Aircraft* 48 (4) (2011) 1204–1211.
1112
1113 321 doi:10.2514/1.C031224.
1114

1121
1122
1123
1124
1125
1126
1127
1128
1129
1130
1131
1132
1133
1134
1135
1136
1137
1138
1139
1140
1141
1142
1143
1144
1145
1146
1147
1148
1149
1150
1151
1152
1153
1154
1155
1156
1157
1158
1159
1160
1161
1162
1163
1164
1165
1166
1167
1168
1169
1170
1171
1172
1173
1174
1175
1176



(a) Wing tip leading edge

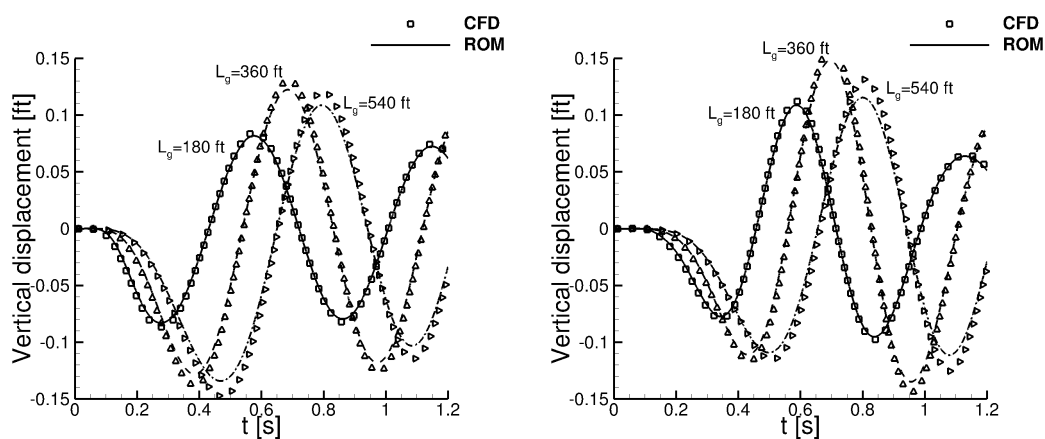
(b) Wing tip trailing edge



(c) Wing tip twist

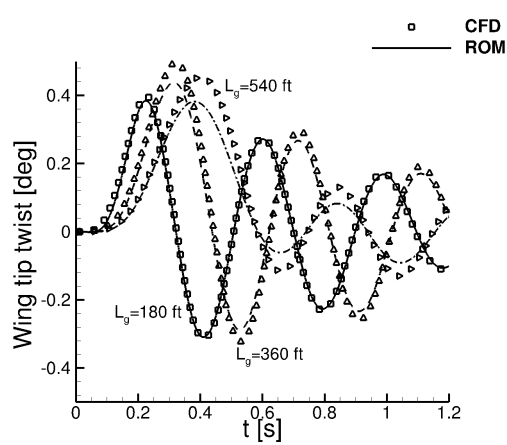
Figure 4: Worst case gust search for the Goland wing/store configuration for a one-minus-cosine gust family (gust intensity 1% of the freestream velocity, Mach 0.85, and altitude 40,000 ft)

1177
1178
1179
1180
1181
1182
1183
1184
1185
1186
1187
1188
1189
1190
1191
1192
1193
1194
1195
1196
1197
1198
1199
1200
1201
1202
1203
1204
1205
1206
1207
1208
1209
1210
1211
1212
1213
1214
1215
1216
1217
1218
1219
1220
1221
1222
1223
1224
1225
1226
1227
1228
1229
1230
1231
1232



(a) Wing tip leading edge

(b) Wing tip trailing edge



(c) Wing tip twist

Figure 5: Gust responses to a one-minus-cosine gust for gust lengths of 180, 360 and 540 ft (gust intensity 1% of the freestream velocity, Mach 0.85, and altitude 40,000 ft)

- 1233
1234
1235
1236
1237
1238
1239
1240 322 [2] V. Parameswaran, J. D. Baeder, Indicial aerodynamics in compressible
1241 323 flow – direct computational fluid dynamic calculations, *Journal of Air-*
1242 324 *craft* 34 (1) (1997) 131–133. doi:10.2514/2.2146.
- 1245 325 [3] Q. Zhou, D. Li, A. D. Ronch, G. Chen, Y. Li, Computational fluid
1246 326 dynamics–based transonic flutter suppression with control delay, *Jour-*
1247 327 *nal of Fluids and Structures* 66 (2016) 183–206. doi:10.1016/j.
1250 328 *jfluidstructs*.2016.07.002.
- 1252 329 [4] K. J. Badcock, S. Timme, S. Marques, H. Khodaparast, M. Prandina,
1253 330 J. E. Mottershead, A. Swift, A. D. Ronch, M. A. Woodgate, Transonic
1254 331 aeroelastic simulation for instability searches and uncertainty analysis,
1255 332 *Progress in Aerospace Sciences* 47 (5) (2011) 392–423. doi:10.1016/j.
1256 333 *paerosci*.2011.05.002.
- 1257 334 [5] M. A. Woodgate, K. J. Badcock, Fast prediction of transonic aeroelastic
1258 335 stability and limit cycles, *AIAA Journal* 45 (6) (2007) 1370–1381. doi:
1259 336 10.2514/1.25604.
- 1260 337 [6] K. J. Badcock, M. A. Woodgate, M. R. Allan, P. S. Beran, Wing-rock
1261 338 limit cycle oscillation prediction based on computational fluid dynamics,
1262 339 *Journal of Aircraft* 45 (3) (2008) 954–961. doi:10.2514/1.32812.
- 1263 340 [7] A. Da Ronch, K. J. Badcock, Y. Wang, A. Wynn, R. N. Palacios, Non-
1264 341 linear model reduction for flexible aircraft control design, in: *AIAA At-*
1265 342 *mospheric Flight Mechanics Conference*, AIAA Paper 2012–4404, Min-
1266 343 neapolis, MN, 2012. doi:10.2514/6.2012-4404.

- 1289
1290
1291
1292
1293
1294
1295
1296 344 [8] N. D. Tantaroudas, A. Da Ronch, K. J. Badcock, R. Palacios, Model or-
1297 345 der reduction for control design of flexible free-flying aircraft, in: AIAA
1298 346 Science and Technology Forum and Exposition, AIAA Paper 2015-0240,
1300 347 Kissimmee, FL, 2015. doi:10.2514/6.2015-0240.
- 1302
1303 348 [9] K. J. Badcock, B. E. Richards, M. A. Woodgate, Elements of compu-
1304 349 tational fluid dynamics on block structured grids using implicit solvers,
1305 350 Progress in Aerospace Sciences 36 (5-6) (2000) 351-392. doi:10.1016/
1307 351 S0376-0421(00)00005-1.
- 1309
1310 352 [10] A. Da Ronch, N. D. Tantaroudas, S. Timme, K. J. Badcock, Model
1312 353 reduction for linear and nonlinear gust loads analysis, in: 54th
1313 354 AIAA/ASME/ASCE/AHS/ASC Structures, Structural Dynamics, and
1314 355 Materials Conference, AIAA Paper 2013-1492, Boston, MA, 2013.
1316 356 doi:10.2514/6.2013-1492.
- 1318
1319 357 [11] S. Timme, K. J. Badcock, A. Da Ronch, Linear reduced order modelling
1321 358 for gust response analysis using the dlr-tau code, in: International Fo-
1322 359 rum on Aeroelasticity and Structural Dynamics (IFASD), IFASD Paper
1324 360 2013-36A, Bristol, U.K., 2013.
- 1326
1327 361 [12] N. D. Tantaroudas, A. Da Ronch, Nonlinear reduced order aeroservoelas-
1328 362 tic analysis of very flexible aircraft, in: P. Marqués, A. Da Ronch (Eds.),
1329 363 Novel Concepts in Unmanned Aircraft Aerodynamics, Flight Stability,
1330 364 and Control, Wiley-Blackwell, Chichester, Great Britain, 2016, ESBN-
1331 365 10: 1118928687, ISBN-13: 978-1118928684.
- 1333
1334
1335
1336 366 [13] K. J. Badcock, H. H. Khodaparast, S. Timme, J. E. Mottershead, Cal-
1337
1338
1339
1340
1341
1342
1343
1344

- 1345
1346
1347
1348
1349
1350
1351
1352 367 culating the influence of structural uncertainty on aeroelastic limit cycle
1353 368 response, in: 52nd AIAA/ASME/ASCE/AHS/ASC Structures, Struc-
1354 369 tural Dynamics, and Materials Conference, AIAA Paper 2011-1741,
1355 370 Denver, CO, 2011. doi:10.2514/6.2011-1741.
1358
1359 371 [14] K. J. Badcock, M. A. Woodgate, Bifurcation prediction of large-order
1360 372 aeroelastic models, AIAA Journal 48 (6) (2010) 1037-1046. doi:10.
1361 373 2514/1.40961.
1364
1365 374 [15] P. S. Beran, N. S. Khot, F. E. Eastep, R. D. Snyder, J. V. Zweber,
1366 375 Numerical analysis of store-induced limit-cycle oscillation, Journal of
1367 376 Aircraft 41 (6) (2004) 1315-1326. doi:10.2514/1.404.
1370
1371 377 [16] S. Timme, S. Marques, K. J. Badcock, Transonic aeroelastic stability
1372 378 analysis using a kriging-based Schur complement formulation, AIAA
1373 379 Journal 49 (6) (2011) 1202-1213. doi:10.2514/1.J050975.
1375
1376 380 [17] P. Bekemeyer, S. Timme, Reduced order gust response simulation using
1377 381 computational fluid dynamics, in: 57th AIAA/ASCE/AHS/ASC Struc-
1378 382 tures, Structural Dynamics, and Materials Conference, AIAA SciTech
1379 383 Forum, AIAA Paper 2016-1485, San Diego, CA, 2016. doi:10.2514/
1380 384 6.2016-1485.
1385
1386
1387
1388
1389
1390
1391
1392
1393
1394
1395
1396
1397
1398
1399
1400